

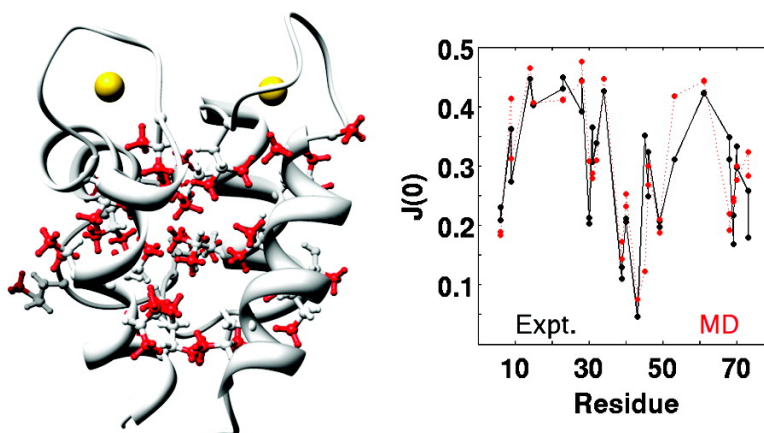
Communication

Toward Quantitative Interpretation of Methyl Side-Chain Dynamics from NMR by Molecular Dynamics Simulations

Scott A. Showalter, Eric Johnson, Mark Rance, and Rafael Brschweiler

J. Am. Chem. Soc., **2007**, 129 (46), 14146-14147 • DOI: 10.1021/ja075976r • Publication Date (Web): 31 October 2007

Downloaded from <http://pubs.acs.org> on February 13, 2009



More About This Article

Additional resources and features associated with this article are available within the HTML version:

- Supporting Information
- Links to the 4 articles that cite this article, as of the time of this article download
- Access to high resolution figures
- Links to articles and content related to this article
- Copyright permission to reproduce figures and/or text from this article

[View the Full Text HTML](#)

Toward Quantitative Interpretation of Methyl Side-Chain Dynamics from NMR by Molecular Dynamics Simulations

Scott A. Showalter,[†] Eric Johnson,[†] Mark Rance,[‡] and Rafael Brüschweiler^{*,†}

Department of Chemistry and Biochemistry & National High Magnetic Field Laboratory, Florida State University, Tallahassee, Florida 32306, and Department of Molecular Genetics, Biochemistry and Microbiology, University of Cincinnati, Cincinnati, Ohio 45267

Received August 8, 2007; E-mail: bruschweiler@magnet.fsu.edu

Advances in molecular dynamics (MD) force fields^{1–3} have recently allowed the nearly quantitative interpretation of protein backbone dynamics as measured by NMR spin relaxation^{4,5} and residual dipolar couplings.⁶ These improvements were solely due to modification of the backbone φ, ψ dihedral angle potential, as implemented in the AMBER99SB² and CHARMM22/CMAP¹ force fields. Amino acid side-chain motions, on the other hand, often play an important functional role, but their accurate simulation has been a considerable challenge in the past.^{7–9}

Because changes in side-chain motions are not necessarily correlated to changes in protein backbone mobility,¹⁰ it is unclear how these force-field modifications affect side-chain dynamics. Here, we compare experimental and simulated side-chain NMR relaxation parameters of calbindin D_{9k} and ubiquitin and report significant improvements in the quantitative representation of side-chain motions by computation.

Methyl groups are the dynamically best studied side-chain moieties of proteins.^{9–15} Deuterium relaxation experiments of ¹³CH₂D methyl groups report on picosecond–nanosecond dynamics and measure up to five different relaxation rates for each methyl group at a given B₀ field.¹⁴ They allow the unambiguous extraction of spectral densities $J(0)$, $J(\omega_D)$, and $J(2\omega_D)$, where ω_D is the Larmor frequency of deuterium. As shown here, these spectral densities lend themselves to direct comparison with computer simulations (Figure 1). Alternatively, model-free dynamics parameters^{14,16,17} can be determined from the experiment first and compared with the corresponding simulated parameters (Figure 2).

Methyl side-chain dynamics of calbindin in its calcium-bound form have recently been reported.¹⁸ Up to five spectral densities $J(\omega)$ have been determined for each of the 37 analyzable methyl groups and interpreted in terms of a model-free analysis.

Here, a 50 ns MD simulation of Ca²⁺-bound calbindin (PDB entry 3ICB¹⁹ with the mutation P34M) was performed using the AMBER 8²⁰ simulation program with the parameter set AMBER99SB following the protocol described previously.⁴ The starting configuration was generated by immersing the calbindin structure in a cubic box with 5778 explicit SPC water molecules and neutralizing counterions. Production dynamics were run at 300 K and 1 atm pressure, with snapshots saved every 1 ps.

The spectral densities $J(\omega) = \int_{-\infty}^{\infty} C(t)\cos(\omega t)dt$ are back-calculated from the trajectory by using the following parametrization of the reorientational time-correlation function $C(t)$ of the methyl C–H bond vectors:

$$C(t) = e^{-t/\tau_c} C_{CC}(t) C_{CH_3}(t) \quad (1)$$

where τ_c is the experimentally determined overall tumbling correlation time, $C_{CC}(t)$ is the reorientational correlation function of

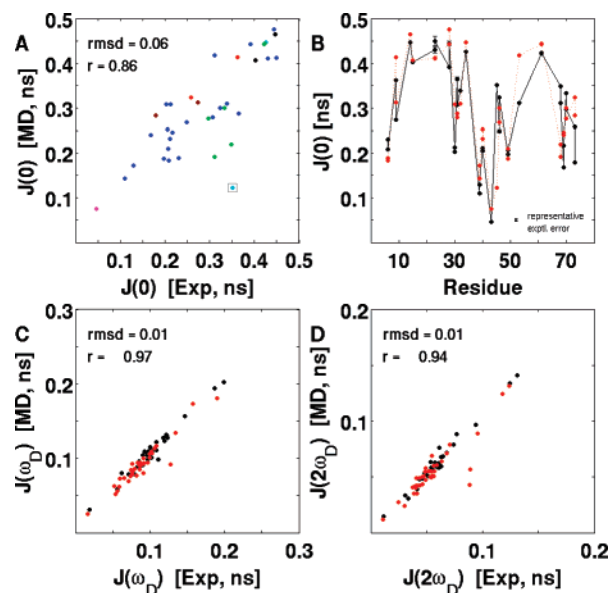


Figure 1. Comparison between experimental¹⁸ and MD back-calculated spectral densities $J(\omega)$ reflecting side-chain dynamics of Ca²⁺-bound calbindin. Where not visible, the experimental error bars are smaller than the symbols. (A) $J(0)$ color coded by residue type: Ala (black), Ile (red), Leu (blue), Met (magenta), Thr (cyan), Val (green). Correlation coefficient excludes Thr45. (B) $J(0)$ as a function of residue number from experiment (black) and MD (red). (C) $J(\omega_D)$ at 500 MHz (black) and 600 MHz (red). (D) $J(2\omega_D)$ at 500 MHz (black) and 600 MHz (red).

the C–C bond that connects the methyl group with the rest of the protein, and $C_{CH_3}(t)$ is the correlation function describing the methyl group rotation itself. Equation 1, which is a modification of the extended model-free approach,^{17,21} factors $C(t)$ into three parts by assuming statistical independence between C–C bond vector reorientation, methyl group rotation, and overall tumbling, which is independently validated by MD (see Supporting Information). The $C_{CC}(t)$ correlation functions were determined after aligning all MD snapshots with respect to the reference snapshot at 25 ns and by fitting the computed correlation function by a sum of five exponentials and an offset.^{4,7} Correlation functions were calculated out to 6 and 12 ns, which is beyond calbindin's isotropic overall tumbling correlation time ($\tau_c = 4.04$ ns). Due to the known difficulty in realistically modeling the correlation time of the methyl group rotation by MD,^{13,15,22} the correlation functions $C_{CH_3}(t)$ were parametrized in a model-free way¹⁶ as $C_{CH_3}(t) = 1/9 + 8/9 \exp(-t/\tau_{CH_3})$ with the methyl rotation correlation times τ_{CH_3} treated as fit parameters to minimize the difference between the simulated and experimental spectral densities $J(\omega)$. Figure 1 shows this comparison for $J(0)$, $J(\omega_D)$, and $J(2\omega_D)$. The agreement for $J(\omega_D)$ and $J(2\omega_D)$ both at 500 MHz (black symbols) and 600 MHz (red

[†] Florida State University.

[‡] University of Cincinnati.

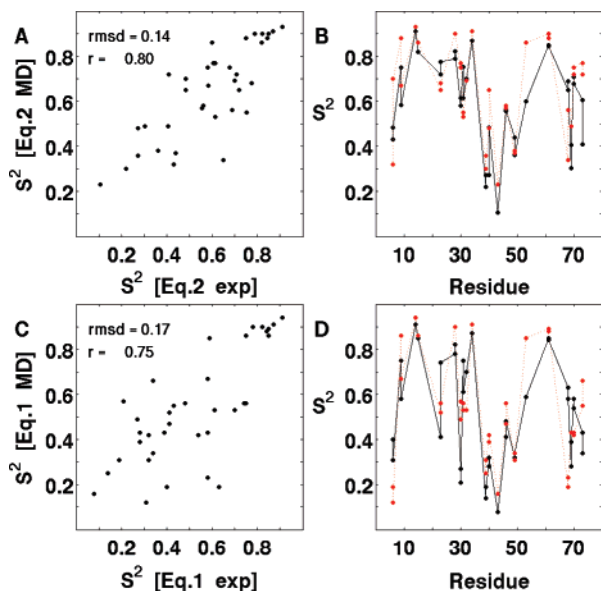


Figure 2. Calbindin methyl order parameters derived from fitting of the experimental spectral densities¹⁸ with correlation functions of eq 2 (A,B) and eq 1 (C,D), compared with order parameters extracted from fitting MD-derived spectral densities to the same equations. (B,D) Black and red circles correspond to experimental and MD S^2 , respectively.

symbols) field strengths (panels C,D) is excellent (correlation coefficients $r \geq 0.94$), partly because of adjusting τ_{CH_3} , whereas for $J(0)$ (panels A,B), the agreement is slightly worse ($r = 0.86$) but still remarkably good considering the high sensitivity of NMR methyl relaxation with respect to the side-chain environment.^{15,22} The rmsd of 0.06 between experimental and simulated $J(0)$ values is smaller than the rmsd between the experimental $J(0)$ of the Ca^{2+} -bound and the apo state. The largest discrepancy is found for Thr45 (boxed data point) whose time correlation function is not well-converged;³ that is, its S^2 value has a low precision (see Supporting Information). On average, the methyl groups of Leu and Ala residues show the best agreement with experiment, whereas the methyl groups of Val and Thr residues deviate most.

Experimentally extracted spectral density functions are often interpreted^{12,14,18} in terms of model-free parameters that enter the functional form¹⁴

$$C_{LS2}(t) = e^{-t/\tau_c} \{ S^2/9 + (1 - S^2/9)e^{-t/\tau_{eff}} \} \quad (2)$$

where τ_{eff} is an effective correlation time for both the methyl group rotation and the reorientational motions of the C–C vector. In Figure 2A,B, the S^2 values obtained by fitting eq 2 to the MD-derived spectral densities are compared with the experimental S^2 values.¹⁸ Alternatively, the expression of eq 1 can be fit to the spectral density data by assuming for the middle term the standard model-free form $C_{CC}(t) = S_{CC}^2 + (1 - S_{CC}^2)\exp(-t/\tau_{CC})$. Figure 2C,D shows the comparison between the S_{CC}^2 order parameters fitted to the experimental and the MD-derived spectral densities, which compare well with a recent contact model for the prediction of methyl order parameters ($r = 0.76$).²³

These results represent a substantial improvement over previous force fields. For example, CHARMM22 simulations without CMAP¹ of TNfn3 and FNfn10 produce correlations with experimental methyl order parameters of $r = 0.62$ and 0.51 .⁸ Similarly, a trajectory of ubiquitin⁴ using AMBER99 yields $r = 0.66$,¹² whereas AMBER99SB yields $r = 0.81$, which is comparable to the agreement found for calbindin (see Supporting Information).

Consistent with the side-chain results, AMBER99SB reproduces backbone N–H order parameters of Ca^{2+} -bound calbindin²⁴ well ($r = 0.86$).

These results demonstrate that the modified backbone potential of AMBER99SB considerably improves the description of amino acid methyl side-chain dynamics, suggesting a direct connection between the accurate representation of the structure (and dynamics) of the protein backbone and side-chain mobility. The benchmarks and the analysis strategy presented here should be useful for the improvement of amino acid side-chain force fields.

Acknowledgment. S.A.S. is the recipient of an NIH postdoctoral fellowship, E.J. of an American Heart Association fellowship. This work was supported by the NIH (Grant GM063855 to M.R.) and NSF (Grant 0621482 to R.B.).

Supporting Information Available: Analysis of MD trajectories of calbindin and ubiquitin. This material is available free of charge via the Internet at <http://pubs.acs.org>.

References

- (1) (a) MacKerell, A. D. *J. Comput. Chem.* **2004**, *25*, 1584–1604. (b) Buck, M.; Bouguet-Bonnet, S.; Pastor, R. W.; MacKerell, A. D. *Biophys. J.* **2006**, *90*, L36–L38.
- (2) (a) Hornak, V.; Abel, R.; Okur, A.; Strockbine, B.; Roitberg, A.; Simmerling, C. *Proteins: Struct., Funct., Bioinf.* **2006**, *65*, 712–725. (b) Hornak, V.; Okur, A.; Rizzo, R. C.; Simmerling, C. *Proc. Natl. Acad. Sci. U.S.A.* **2006**, *103*, 915–920.
- (3) Yang, W.; Nymeyer, H.; Zhou, H.-X.; Berg, B.; Brüschweiler, R. *J. Comput. Chem.* **2007**, in press.
- (4) Showalter, S. A.; Brüschweiler, R. *J. Chem. Theory Comput.* **2007**, *3*, 961–975.
- (5) Markwick, P. R. L.; Bouvignies, G.; Blackledge, M. *J. Am. Chem. Soc.* **2007**, *129*, 4724–4730.
- (6) Showalter, S. A.; Brüschweiler, R. *J. Am. Chem. Soc.* **2007**, *129*, 4158–4159.
- (7) Bremi, T.; Brüschweiler, R.; Ernst, R. R. *J. Am. Chem. Soc.* **1997**, *119*, 4272–4284.
- (8) Best, R. B.; Clarke, J.; Karplus, M. *J. Mol. Biol.* **2005**, *349*, 185–203.
- (9) (a) Skrynnikov, N. R.; Millet, O.; Kay, L. E. *J. Am. Chem. Soc.* **2002**, *124*, 6449–6460. (b) Zhuravleva, A.; Korzhnev, D. M.; Nolde, S. B.; Kay, L. E.; Arseniev, A. S.; Billeter, M.; Orekhov, V. Y. *J. Mol. Biol.* **2007**, *367*, 1079–1092.
- (10) (a) Lee, A. L.; Kinnear, S. A.; Wand, A. J. *Nat. Struct. Biol.* **2000**, *7*, 72–77. (b) Fuentes, E. J.; Der, C. J.; Lee, A. L. *J. Mol. Biol.* **2004**, *335*, 1105–1115.
- (11) (a) Nicholson, L. K.; Kay, L. E.; Baldisseri, D. M.; Arango, J.; Young, P. E.; Bax, A.; Torchia, D. A. *Biochemistry* **1992**, *31*, 5253–5263. (b) Nicholson, L. K.; Kay, L. E.; Delaglio, F.; Bax, A.; Torchia, D. A. *Biophys. J.* **1993**, *64*, A182–A182. (c) Ishima, R.; Louis, J. M.; Torchia, D. A. *J. Mol. Biol.* **2001**, *305*, 515–521. (d) Ishima, R.; Petkova, A. P.; Louis, J. M.; Torchia, D. A. *J. Am. Chem. Soc.* **2001**, *123*, 6164–6171. (e) Sprangers, R.; Kay, L. E. *Nature* **2007**, *445*, 618–622.
- (12) Wand, A. J.; Urbauer, J. L.; McEvoy, R. P.; Bieber, R. J. *Biochemistry* **1996**, *35*, 6116–6125.
- (13) Chatfield, D. C.; Szabo, A.; Brooks, B. R. *J. Am. Chem. Soc.* **1998**, *120*, 5301–5311.
- (14) (a) Millet, O.; Muhandiram, D. R.; Skrynnikov, N. R.; Kay, L. E. *J. Am. Chem. Soc.* **2002**, *124*, 6439–6448. (b) Kay, L. E. *J. Magn. Reson.* **2005**, *173*, 193–207.
- (15) Xue, Y.; Pavlova, M. S.; Ryabov, Y. E.; Reif, B.; Skrynnikov, N. R. *J. Am. Chem. Soc.* **2007**, *129*, 6827–6838.
- (16) (a) Lipari, G.; Szabo, A. *J. Am. Chem. Soc.* **1982**, *104*, 4546–4559. (b) Lipari, G.; Szabo, A. *J. Am. Chem. Soc.* **1982**, *104*, 4559–4570.
- (17) Clore, G. M.; Szabo, A.; Bax, A.; Kay, L. E.; Driscoll, P. C.; Gronenborn, A. M. *J. Am. Chem. Soc.* **1990**, *112*, 4989–4991.
- (18) Johnson, E.; Chazin, W. J.; Rance, M. *J. Mol. Biol.* **2006**, *357*, 1237–1252.
- (19) Szebenyi, D. M. E.; Moffat, K. *J. Biol. Chem.* **1986**, *261*, 8761–8777.
- (20) Case, D. A.; Cheatham, T. E.; Darden, T.; Gohlke, H.; Luo, R.; Merz, K. M.; Onufriev, A.; Simmerling, C.; Wang, B.; Woods, R. J. *J. Comput. Chem.* **2005**, *26*, 1668–1688.
- (21) Lee, A. L.; Flynn, P. F.; Wand, A. J. *J. Am. Chem. Soc.* **1999**, *121*, 2891–2902.
- (22) Chatfield, D. C.; Augsten, A.; D’Cunha, C. *J. Biomol. NMR* **2004**, *29*, 377–385.
- (23) Ming, D. M.; Brüschweiler, R. *J. Biomol. NMR* **2004**, *29*, 363–368.
- (24) (a) Kördel, J.; Skelton, N. J.; Akke, M.; Palmer, A. G.; Chazin, W. J. *Biochemistry* **1992**, *31*, 4856–4866. (b) Akke, M.; Skelton, N. J.; Kördel, J.; Palmer, A. G.; Chazin, W. J. *Biochemistry* **1993**, *32*, 9832–9844.

JA075976R